이학석사학위논문

PKA에 의한 예쁜꼬마선충 ATGL-1 단백질 양적 조절

PKA regulates ATGL-1 protein level in *C. elegans*

2013년 8월

서울대학교 대학원

생명과학부

장 주 연

PKA에 의한 예쁜꼬마선충 ATGL-1 단백질 양적 조절

PKA regulates ATGL-1 protein level in *C. elegans*

지도교수 김 재 범

이 논문을 이학석사학위논문으로 제출함

2013년 8월

서울대학교 대학원

생명과학부

장 주 연

장주연의 이학석사 학위논문을 인준함

2013년 8월

위 원 장 _____ (인)

부 위 원 장 _____ (인)

위 원 _____ (인)

PKA regulates ATGL-1 protein level in *C. elegans*

A dissertation submitted in partial fulfillment of

the requirement for the degree of

MASTER OF SCIENCE

to the Faculty of the

School of Biological Sciences

at

SEOUL NATIONAL UNIVERSITY

by

Ju Yeon Jang

Date Approved:

_____ _____

_____

_____

ABSTRACT

PKA regulates ATGL-1 protein level in *C. elegans*

Ju Yeon Jang

School of Biological Sciences

The Graduate School

Seoul National University

Fasting-induced lipolysis plays a crucial role to provide energy source by hydrolyzing stored lipid metabolites. In *C. elegans*, both ATGL-1 and PKA are well conserved and mediate lipolysis. Previous studies have suggested that PKA is involved in the regulation of ATGL activity. However, the regulatory mechanism of ATGL-1 and its relationship with PKA are largely unknown in *C. elegans*. In this study, I demonstrate that ATGL-1 is a key lipase for PKA-mediated fasting lipolysis and PKA phosphorylates ATGL-1 at serine 303. Furthermore, I reveal that phosphorylation of ATGL-1 regulates the level of ATGL-1 protein. It is of note that the phosphorylation-dependent ATGL-1 protein is associated with the regulation of ATGL-1 protein stability, although it cannot be ruled out that other mechanisms might contribute to this process. Taken together, I propose a novel regulatory mechanism of ATGL-1 protein by PKA, which appears to be important for ATGL-1-mediated lipolysis upon fasting in *C. elegans*.

Key words: ATGL-1, PKA, phosphorylation, protein level regulation

Student number: 2011-23260

TABLE OF CONTENTS

LIST OF TABLES

LIST OF FIGURES

INTRODUCTION

Animals are able to store excess energy in the form of triglyceride (TG) in cytosolic lipid droplets (LDs). In most mammals, white adipose tissue (WAT) is thus far known to be the most efficient, major organ of fat storage (Zimmerman *et al*, 2009). LD is well developed in adipocytes of adipose tissue than in nonadipocytes; the white adipocyte contains a huge unilocular lipid droplet whereas those in nonadipocytes are much smaller and multilocular (Ohsaki *et al*, 2009). LDs consist of a TG and cholesterol ester core and are surrounded by a phospholipid monolayer embedded with various proteins of different functions (Brasaemle *et al*, 2004; Liu *et al*, 2004). LD formation and breakdown are actively and dynamically regulated in response to nutrient availability. In fed state, the continuous supply of fatty acids lead to synthesis of TG in the endoplasmic reticulum (ER). It is believed that nascent lipid droplets are formed in the ER by lipid accumulation either between the two leaflets of the ER membrane or on the cytosolic surface of the ER (Murphy *et al*, 1999; Robenek *et al*, 2006). There are several hypotheses as to how lipid droplets grow and store lipid once they are made in the ER. Lipid droplets might enlarge either by being permanently attached to the ER, fusing with other lipid droplets, or synthesizing TG on lipid droplet surface (Fujimoto *et al*, 2007). On the other hand, in times of fasting, the stored TG is hydrolyzed by cellular TG hydrolases in response to several hormones such as glucagon (Heckemeyer *et al*, 1983; Slavin *et al*, 1994; Perea *et al*, 1995) and glucocorticoids (Xu *et al*, 2009; Fain *et al*, 1970; Slavin *et al*, 1994). In adipose tissue, free fatty acids (FFAs) and glycerols released upon

lipolysis are delivered to other tissues with high energy demand such as skeletal muscle.

During nutritional deprivation, activation of β-adrenergic receptors by catecholamines plays a key role to turn on catabolic pathways by increasing cAMP levels (Steinberg *et al*, 1972). Increased cAMP in turn activates protein kinase A (PKA), which acts as an important master regulator of fasting lipolysis by phosphorylating and activating perilipin and hormone sensitive lipase (HSL). For many decades, HSL has been considered as a major TG hydrolase among several lipases during nutritional deprivation. However, in 2004, three groups independently identified a novel triglyceride lipase in WAT and named it as adipose triglyceride lipase (ATGL) (Zimmermann *et al*, 2004), desnutrin (Villena *et al*, 2004), or phospholipase A2ξ (Jenkins *et al*, 2004). Recent studies have proposed that ATGL governs lipid catabolism with several other proteins. ATGL activity is regulated by binding with a coactivator called α/β hydrolase domain containing protein 5 [ABHD5; also known as comparative gene identification-58 (CGI-58)] (Lass *et al*, 2006). Under basal state, CGI-58 is bound to perilipin at surface of LD; upon fasting, activated PKA phosphorylates perilipin, by which CGI-58 is released, binds to ATGL in the cytosol, and activates and recruits it to the LD surface (Granneman *et al*, 2007; Yamaguchi *et al*, 2004; Subramanian *et al*, 2004; Lass *et al*, 2006). However, besides binding with CGI-58, other regulatory mechanisms of ATGL have not been clearly elucidated.

During fasting lipolysis, PKA has been well established to directly activate HSL and perilipin. However, there have been controversies as to whether or not PKA directly regulates ATGL. For many years, it has been proposed that only HSL and perilipin are phosphorylated by PKA during lipolysis. Although ATGL has been known to be

phosphorylated on two conserved residues (serine 404 and 428), the responsible kinase(s) and the effect of phosphorylation on the enzyme function have been unclear (Bartz *et al*, 2007). While PKA has been excluded as the kinase responsible for ATGL phosphorylation (Zimmermann *et al*, 2004), Pagnon *et al*. very recently showed that PKA phosphorylates ATGL at serine 406 (murine) or serine 404 (human), both *in vitro* and *in vivo* (Pagnon *et al*, 2012). Also, Pagnon *et al*. have observed increased ATGL serine 406 phosphorylation upon fasting and β-adrenergic stimulation (Pagnon *et al*, 2012). Furthermore, they have reported decreased TG hydrolase activity and lipolytic rate with ATGL phosphorylation mutant (ATGL S406A).

C. elegans is a powerful genetic model system that has been mainly used in studies of development and lifespan due to its various advantages such as short lifespan and easiness of genetic manipulation, and it has recently begun to be used in the field of lipid metabolism as well. *C. elegans* is able to accumulate lipid metabolites in the intestine and the hypodermis (Schroeder *et al*, 2007; Mullaney and Ashrafi, 2009), and the stored lipid metabolites can be readily visualized with various staining dyes including Oil Red O (Sourkas *et al*, 2009; O'Rourke *et al*, 2009). Furthermore, many of the mammalian genes involved in fasting lipolysis are well conserved in *C. elegans*. For instance, ZK909.2 (kin-1) and R07E4.6 (kin-2), catalytic and regulatory subunits of PKA, respectively, are conserved and involved in fasting lipolysis, as PKA-hyperactivated KG532 mutant worms show decreased amount of lipid metabolites both in fed and fasted states compared to wild type (unpublished data). There are three homologous genes of ATGL – C05D11.7, B0524.2, and D1054.1– in *C. elegans*, out of which C05D11.7 (Atgl-1) bears the highest sequence homology to mammalian ATGL (approximately 45%) and

is most studied. It has been shown that atgl-1 is modulated by aak-1 (AMPK) in lipid mobilization (Narbonne *et al*, 2008) and mediates fasting lipolysis (unpublished data). Recently, a sequence homolog of CGI-58, C25A1.12, has been demonstrated to be involved in fasting lipolysis as well and named as LID-1 (Lipid Droplet protein-1) by our group (unpublished data). Since the key metabolic pathways and their regulators are largely conserved, studying lipid metabolism in *C. elegans* can be very informative. However, the actual functions and roles of the lipolytic proteins in lipolysis are not fully understood yet. Moreover, the lipolytic machinery of *C. elegans* appears to be not entirely similar with the mammalian one. For example, *C. elegans* lacks perilipin or any kind of PAT domain-containing lipid droplet protein. Additionally, although there is a *C. elegans* homolog of HSL, C46C11.1 (hosl-1), it has been shown by our group to have minimal role in fasting lipolysis, unlike in mammals (unpublished data). Therefore, there might be a novel regulatory mechanism of ATGL-1 in *C. elegans* that is different from that in mammals.

In this study, I demonstrate that KIN-1 and KIN-2 (hereafter referred to as PKA for simplicity) are key upstream factors of ATGL-1 and activate lipolysis via ATGL-1 upon fasting in *C. elegans*. Furthermore, PKA directly regulates ATGL-1 protein level via phosphorylation, and this ATGL-1 protein level regulation is partly mediated by proteasome degradation. Taken together, these data suggest that PKA phosphorylates ATGL-1 and regulates its protein amount by increasing protein stability in *C. elegans*.

MATERIALS AND METHODS

C. elegans maintenance

Nematodes were cultured on OP50 bacterial lawns on nematode growth media (NGM) plates at 20°C. N2 Bristol was used as the wild-type strain, and the strains VS20 hjIs67[Patgl-1::*atgl-1*::gfp] and KG532 *kin-2(ce179)* were obtained from the *Caenorhabditis* Genetics Center (Minneapolis, MN, USA).

RNAi

Before feeding RNAi, worms were synchronized by hypochlorite treatment of gravid adults. Worms were fed HT115 E. coli strains expressing RNAi constructs as previously described (Timmons and Fire, 1998). The empty vector (L4440) was used as a negative control, and the L4440 and C05D11.7 (atgl-1) HT115 strains were obtained from the Ahringer *C. elegans* RNAi library.

Cell culture

Human embryonic kidney 293T (HEK 293T) cells were maintained in Dulbecco's modified Eagle's medium (DMEM, Hyclone, USA) supplemented with 10% (v/v) fetal bovine serum (FBS, Hyclone) and 1% antibiotic-antimycotic (AA, Hyclone)/penicillin-streptomycin (PS, Hyclone) solution at 5% C) at 37˚C.

Transient transfection

For transfection of expression plasmid, HEK293T cells were grown to 70% confluence in 100 mm or 12-well plate. Each expression plasmid (4 μg or 0.8 μg) was transfected into cells using Lipofectamine™ 2000 (Invitrogen, CA) according to the manufacturer's protocol. After 4 hours post-transfection, the medium was replaced with DMEM supplemented with 10% FBS and 1% AA/PS. For protein amount test, after 24 hours post-transfection, 20 μM forskolin (FSK, Calbiochem)or equal amount of dimethyl sulfoxide (DMSO, Amresco) in serum-free DMEM media was treated to corresponding plates. As for protein stability test, 20 μM forskolin (FSK, Calbiochem) alone,20 μM MG132 (Calbiochem) alone, 20 μM forskolin and 20 μM MG132, or equal amount of dimethyl sulfoxide (DMSO, Amresco) were treated to corresponding plates 24 hours post-transfection. After incubation for 4 hours, cells were harvested.

RNA isolation and quantitative RT-PCR analysis

Total RNA was isolated by using Trizol®Reagent (Invitrogen, CA) according to the manufacturer's protocol. The complementary DNA was synthesized using M-MuL V reverse transcriptase with random hexamer primer (Fermentas, MD). Quantitative RT-PCR (qRT-PCR) was performed on a CFX96 Real time system (Bio-Rad, CA) with SYBR Green (Invitrogen, CA). Relative expression levels of all mRNA were normalized by the level of actin-1/3 mRNA. Primer sequences for qRT-PCR are shown in Table 1.

Phosphorylation site prediction

The amino acid sequence of C05D11.7a, isoform a of *C. elegans* ATGL-1, as provided by WormBase, was analyzed by GPS2.1 software for potential PKA

phosphorylation sites. The corresponding kinase was set as AGC/PKA and the threshold as medium. The resulting potential sites were aligned by score and the serine residue with the highest prediction score was selected.

Expression plasmids

The isoform a of ATGL-1 ORF, encoding amino acids 1 to 621 of *C. elegans* ATGL-1, was cloned into the pPD95.77 plasmid (Addgene) and p3xFLAG-CMV^{TM}-10 plasmid (Sigma Aldrich). Mutant plasmids were made by site-directed mutagenesis using ATGL-1-pPD95.77 construct for microinjection and ATGL-1- p3xFLAG-CMV^{TM}-10 construct for transient transfection. The AGT sequence encoding serine 303 of ATGL-1 was changed as follow: A to G and G to C for S303A mutant, and A to G and G to A for S303D mutant. Primer sequences for mutagenesis are also shown in Table 2.

Generation of GFP fusion transgenic animals and image acquisition

Wild type (WT) or phosphorylation mutant (S303A or S303D) ATGL-1-pPD95.77 purified plasmid was diluted to 10 ng/ul and rol-6 to 100 ng/ul. The purified plasmid solution was injected into capillary tube (GD-1, 1X90mm) using Plain Glass Capillary tube (I.D. 1.1~1.2mm, length 75mm) attached to mouth pipette. The capillary tube was connected to Femtoget (Eppendorf) and a young adult *C. elegans* was fixed on agar pad with halocarbon. The plasmid DNA solution was injected into the distal gonad of the worm. The worm was dissolved in M9 buffer (0.3% (w/v) KH_2PO_4, 0.6% (w/v) Na_2HPO_4, 0.5% (w/v) NaCl, and 1M $MgSO_4$) and transferred to a new NGM plate. 15 to 20 worms were injected for each construct. F1 offspring with rol-6 phenotype were

observed about 5 days post-microinjection and each F1 transgenic worm was transferred to one NGM plate. The transgenic mutants were grown for over three generations until a stable transgenic line was established.

The GFP fluorescence was visualized using a Zeiss Axio Observer Z1 microscope equipped with Zeiss LSM 700 confocal unde rEGFP and Nile Red filters. For image analyses, images were captured using Zeiss Zen 2009 software. All GFP images were obtained under identical settings and exposure times for direct comparisons.

GST pull-down assay

GST-tagged ATGL-1 was amplified in and purified from BL21 strain bacteria. Each of the *in vitro* translated proteins was mixed with GST-ATGL-1 fusion protein encoding the *C. elegans* ATGL-1, which was bound to glutathione-sepharose beads. Reaction beads were made up to 200 ul with binding buffer (10 mM Tris-HCl [pH 7.4], 100 mM NaCl, 1 mM EDTA, 1 mM DTT, 1 mM PMSF, 1% (v/v) NP-40 and protease inhibitor cocktail) and incubated for 3 hours at 4˚C. The beads were washed three times with binding buffer and analyzed by autoradiography after SDS-PAGE.

In vitro kinase assay

Mammalian PKA (New England Biolabs, MA), 10X kinase buffer (500 mM Tris-HCl [pH 7.5], 1mM EGTA, 100 mM magnesium acetate), ^{32}P-labeled 1mM ATP, 5 ul of sample DNA, and distilled water were mixed up to 25 ul and incubated for 30 minutes at 37˚C. The kinase reaction was analyzed by autoradiography after SDS-PAGE and coomassie staining.

Western blotting and Image Quantitation

The cells were lysed on ice with radioimmunoprecipitation assay (RIPA) buffer (50 mM Tris-HCl [pH 7.4], 150 mM NaCl, 1 mM EDTA, 1 mM PMSF, 1% (v/v) NP-40, 0.25% (w/v) Na-deoxycholate and protease inhibitor cocktail) and subjected to Western blotting. Proteins were boiled in SDS sample buffer for 5 minutes, separated on SDS-PAGE and transferred to polyvinylidenedifluoride (PVDF) membranes (Millipore, Temecula, CA, USA). Blots were blocked 5% (g/v) skim milk in Tris-buffered saline containing 0.1% (v/v) Tween-20 (TBST, 25 mM Tris-Hcl [pH 8.0], 137 mM NaCl, 2.7 mM KCl and 0.1% Tween-20) at room temperature for 30 minutes, followed by overnight incubation with primary antibodies at 4˚C. Antibodies against β-actin (Sigma-Aldrich), Flag-tag (Sigma-Aldrich), and Myc-tag (Sigma-Aldrich) were used. After being washed with TBST three times, the blots were hybridized with secondary antibodies conjugated with horseradish peroxidase (Sigma-Aldrich) in 5% skim milk dissolved in TBST at room temperature for 2 hours and additionally washed three times with TBST. The membranes were then incubated with enhanced chemiluminescence reagents and quantified with LuminoImager (LAS-3000) and Science Lab Image Gauge software (Fuji Photo Film).The band intensities of the lanes were quantified using the Image J software (NIH).

Oil Red O staining, Image Acquisition and Quantitation

100~200 worms are collected at young adult stage and washed twice with distilled water or M9 buffer to cleanse any remnant bacteria. Add 60μl of PBS, 60μl of 4% paraformaldehyde, and 120 μl of 2X MRWB and freeze instantly with liquid nitrogen.

The worms are frozen-thawed for three times and washed with 1 ml of PBS. The worms are dehydrated with 1 ml of 60% isopropyl alcohol for 10 minutes at room temperature and washed with 1 ml of PBS. They are stained with 700 to 800 μl of 60% Oil Red O for 30 minutes at room temperature. Oil Red O images were captured using a digital CCD camera (Zeiss AxioCamHRc) attached to a Zeiss Axioplan2 Imaging. All Oil Red O images were obtained under identical settings and exposure times for direct comparisons. The relative Oil Red O intensities of the intestinal cells were quantified using the Image J software (NIH), and 8-10 worms from each genotype were randomly selected for the quantification.

Statistical analysis

All data were presented as mean ± standard deviation (S.D.). The *p* value was analyzed using the Student's t test. Differences were considered as statistically significant at *, #$p<0.05$ and **, ##$P<0.01$.

Table 1

qRT-PCR primers			
Gene	**Species**	**Forward**	**Reverse**
atgl-1	*C. elegans*	5'-GAGATCGCCGAAGAAAGTTG-3'	5'-TGCTGATGTTGTGATGCTGA-3'
actin-1/3	*C. elegans*	5'-TCGTCCTCGACTCTGGAGAT-3'	5'-GCCATTTCTTGCTCGAAGTC-3'
kin-2 (3' UTR)	*C. elegans*	5'-ATCCAGCATTGCGAAGTCTC-3'	5'-GGGGAAACCGACAAAAAGTT-3'
kin-2 (2nd exon)	*C. elegans*	5'-GCAACGACACAACATTCAGC-3'	5'-GGGTTGTCGGGTTTGTGTAT-3'
cpt-3	*C. elegans*	5'-GGAGGAAGGATTGGAGGAAG-3'	5'-CACATACGAGCTTGCAGGAA-3'
fat-7	*C. elegans*	5'-ACGAGCTTGTCTTCCATGCT-3'	5'-ATCCACGGGTGGTGTTATGT-3'

Table 2

Cloning & mutagenesis primers		
Construct	**Forward**	**Reverse**
S303A	5'-CGAATGAAGAAACGTGCGGCTGCAAATGCTTTGAACAG-3'	5'-CTGTTCAAAGCATTTGCAGCCGCACGTTTCTTCATTCG-3'
S303D	5'-CGAATGAAGAAACGTGCGGATGCAAATGCTTTGAACAG-3'	5'-CTGTTCAAAGCATTTGCATCCGCACGTTTCTTCATTCG-3'

RESULTS

C. elegans ATGL-1 is downstream of PKA during lipolysis

In mammals, it has been well established that ATGL plays a crucial role in PKA-mediated lipolysis (Zimmerman *et al*, 2004; Steinberg *et al*, 2007). Our group has shown that ATGL-1 is the key lipase responsible for fasting lipolysis in *C. elegans*, whereas other lipases such as HOSL-1 (homolog of HSL) do not contribute to fasting lipolysis (unpublished data). However, the relationship between PKA and ATGL-1 has not been clearly elucidated in *C. elegans*. To investigate this, I used atgl-1 RNA interference in wild type (N2) or KG532 strains, in which kin-2 loss-of-function by missense mutation of arginine 92 (R92C) causes PKA hyperactivation. The amounts of accumulated lipid metabolites were visualized by Oil Red O staining to decipher the relationship between PKA and ATGL-1 in lipolysis.

Under basal state, KG532 mutant demonstrated reduced lipid amounts compared to wild type (N2) worms (Fig. 1A and B). As previously observed, the fat content of N2 worm was slightly increased when atgl-1 was knocked down (Fig. 1A and B), confirming the positive role of ATGL-1 in lipolysis. Interestingly, upon atgl-1 knockdown, the fat content of KG532 mutant was restored to a level similar to that of wild type worms (Fig. 1A and B), implying that ATGL-1 would mediate PKA-induced lipolysis. Therefore, it is likely that in *C. elegans* PKA would be an upstream factor of ATGL-1 and both PKA and ATGL-1 are involved in lipolysis.

Figure 1. ATGL-1 is downstream of PKA in C. elegans lipolysis.

Representative images of Oil Red O staining of N2 wild type and KG532 mutants upon atgl-1 knockdown. (A) Gravid N2 and KG532 worms were synchronized and grown on control L4440 or atgl-1 RNAi plates for 2 to 3 days. Approximately 200 worms were fixed with PBS, 4% paraformaldehyde, and 2X MRWB and stained with 60% Oil Red O for 30 minutes for each group. Images were obtained under identical settings and exposure time. (B) Relative Oil Red O intensities of the intestine were quantified using Image J software (NIH). Values are mean ± S.D. ($n \geq 5$ for each group). *$p<0.05$, **$P<0.01$ versus other strain, #$p<0.05$, ##$P<0.01$ versus same strain on atgl-1, Student′s t-test.

Figure 1

A

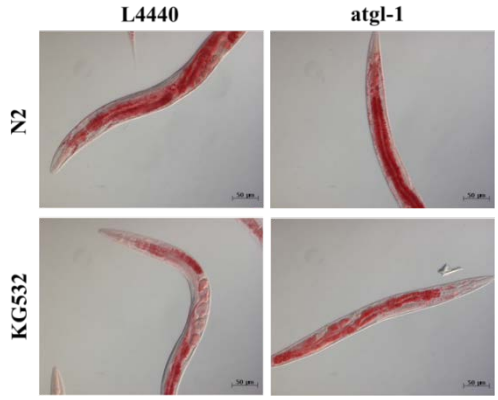
L4440
atgl-1
N2
KG532

B

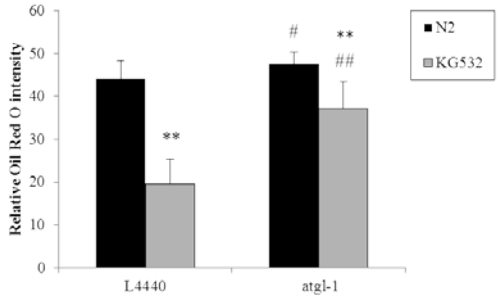
Relative Oil Red O intensity
60
50
40
30
20
10
0
**
#
**
##
L4440
atgl-1
N2
KG532

PKA regulates ATGL-1 primarily at protein level

Although PKA is known to be an upstream factor of ATGL in mammals, it is unclear whether PKA directly regulates ATGL-1. Therefore, to investigate whether PKA would modulate ATGL-1 in *C. elegans*, I suppressed kin-2 via RNAi in ATGL-1 transgenic VS20 strain [ATGL-1p::ATGL-1::GFP], which is a useful model to monitor ATGL-1 protein by GFP fluorescence. Kin-2 RNAi decreased kin-2 mRNA by approximately 50% (Fig. 2C). Under basal condition, ATGL-1::GFP was detected as dot-like puncta, and upon kin-2 knockdown, the amount of ATGL-1::GFP puncta was clearly and significantly increased (Fig. 2A). However, the mRNA level of ATGL-1::GFP was not increased as significantly as the protein level (Fig. 2B), indicating that PKA might directly regulate ATGL-1 primarily at protein level rather than at mRNA level. To observe the change in ATGL-1 mRNA level in a physiological condition, N2 worms were fasted for 2.5 hours, in which PKA was assumed to be activated by fasting signals. The fasting status was confirmed by the mRNA expressions of various fasting responsive genes such as fil-1, fil-2, and cpt-3(Fig. 3E-G). The mRNA level of endogenous ATGL-1 was observed to remain relatively constant upon fasting for 2.5 hours (Fig. 2C), increasing the possibility that ATGL-1 is regulated by PKA mainly at protein level.

PKA phosphorylates ATGL-1 mainly at serine 303

Although some studies have shown that PKA does not phosphorylate ATGL, it has been very recently reported that mammalian ATGL is phosphorylated by PKA (Zimmerman *et al.*, 2004; Pagnon*et al*., 2012). Therefore, I further investigated whether PKA regulation of ATGL-1 at protein level is via direct phosphorylation. First, I analyzed

Figure 2. PKA activation primarily increases ATGL-1 protein expression.

(A) ATGL-1::GFP of VS20 mutants upon kin-2 knockdown. Images were obtained using Zeiss Axio Observer Z1 microscope equipped with Zeiss LSM 700 confocal under EGFP and Nile Red filters. For image analyses, images were captured using Zeiss Zen 2009 software. All images were obtained under identical settings and exposure times. (B) through (G) Total RNA was extracted from VS20 and N2 worms using Trizol® Reagent (Invitrogen, CA) according to the manufacturer′s protocol and each mRNA level was normalized by actin-1/3 mRNA level. (B and C) Atgl-1 mRNA level of VS20 mutants upon kin-2 knockdown is shown in (B), kin-2 mRNA level in (C). (D through G) Atgl-1 (C), fil-1 (D), fil-2 (E), and cpt-3 (F) mRNA levels of N2 worms upon fasting for 2.5 hours are shown. Values are mean ± S.D. (n=3 for each group). #$p<0.05$, ##$P<0.01$ versus same strain on atgl-1, Student′s t-test.

Figure 2

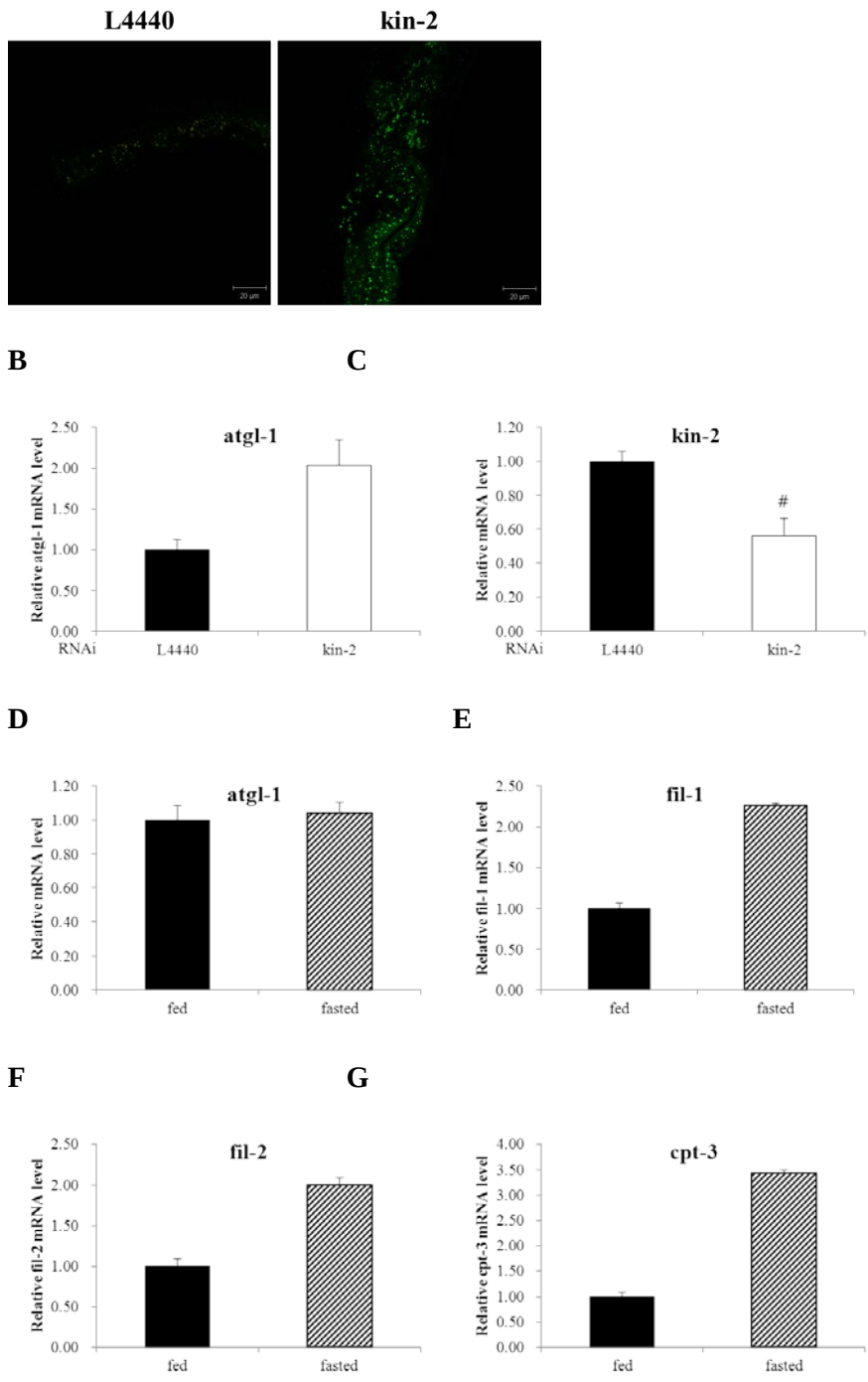
A
L4440
kin-2
B
atgl-1
Relative atgl-1 mRNA level
2.50
2.00
1.50
1.00
0.50
0.00
RNAi
L4440
kin-2
C
kin-2
Relative mRNA level
1.20
1.00
0.80
0.60
0.40
0.20
0.00
#
RNAi
L4440
kin-2
D
atgl-1
Relative mRNA level
1.20
1.00
0.80
0.60
0.40
0.20
0.00
fed
fasted
E
fil-1
Relative fil-1 mRNA level
2.50
2.00
1.50
1.00
0.50
0.00
fed
fasted
F
fil-2
Relative fil-2 mRNA level
2.50
2.00
1.50
1.00
0.50
0.00
fed
fasted
G
cpt-3
Relative cpt-3 mRNA level
4.00
3.50
3.00
2.50
2.00
1.50
1.00
0.50
0.00
fed
fasted

the amino acid sequence of ATGL-1 isoform a, as provided by WormBase, by GPS2.1 software (Xue *et al*., 2008) to find potential PKA phosphorylation sites. Among several potential sites, serine 303 revealed the highest prediction score (Fig. 3A, left panel) and it matched one of the known PKA consensus motifs, R-X-S*/T* (Fig. 3A, right panel), as previously described (Kennelly and Krebs, 1991). In order to confirm that serine 303 is indeed a PKA phosphorylation site, I mutated it to alanine by site-directed mutagenesis to generate phosphorylation-defective form of atgl-1 (S303A).

Next, I performed *in vitro* kinase assay with GST-tagged recombinant WT or S303A ATGL-1. As shown in Figure 3B, WT ATGL-1 was strongly phosphorylated by PKA while S303A ATGL-1 was not in *in vitro* kinase assay. Thus, these data suggest that serine 303 might be one of the major PKA phosphorylation sites of ATGL-1. However, I cannot rule out the possibility that other serine/threonine residues may also be phosphorylated and contribute to the regulation of ATGL-1 by PKA.

Phosphorylation at serine 303 regulates ATGL-1 protein expression

Since the amount of ATGL-1::GFP puncta increased upon kin-2 knockdown in VS20 mutant (Fig. 2A), I hypothesized that ATGL-1 protein level might be regulated by PKA phosphorylation. To test this hypothesis, I generated phosphorylation-defective form (S303A) as well as phosphomimic form (S303D) of ATGL-1 by site-directed mutagenesis. Next, I overexpressed WT, S303A, and S303D atgl-1 in mammalian HEK 293T cells with or without forskolin treatment since forskolin is a potent PKA activator.

Upon forskolin treatment, WT atgl-1 protein level was greatly increased (Fig. 4A and B), recapitulating the effect of kin-2 knockdown on ATGL-1::GFP level in VS20

Figure 3. PKA phosphorylates ATGL-1 at serine 303.

(A) The amino acid sequence of ATGL-1 isoform a, as provided by WormBase, was analyzed by GPS2.1 software (Xue et al., 2008) to find potential PKA phosphorylation sites. Top five potential phosphorylation sites of ATGL-1, aligned from highest to lowest score, are shown at left. PKA consensus motifs as previously described (Kennelly and Krebs, 1991) are shown at right. (B) Mammalian PKA, 10X kinase buffer, ^{32}P-labeled 1 mM ATP, 5 μl of sample DNA (free GST and wild type and S303A GST-labeled ATGL-1), and distilled water were mixed up to 25 μl and incubated for 30 minutes at 37˚C. Autoradiography of WT and S303A ATGL-1 *in vitro* kinase assay and the corresponding Coomassie blue-stained SDS-PAGE gel are shown.

Figure 3

A

Position	Code	Kinase	Peptide	Score
303	S	AGC/PKA	PRMKKRASANALNSF	5.049
316	S	AGC/PKA	SFRTRGESECETCGD	2.530
81	T	AGC/PKA	VSQARSRTFGPLHPE	2.495
303	S	AGC	PRMKKRASANALNSF	2.416
369	T	AGC/PKA	FRLVRYATTAMGISK	2.403

PKA consensus motif
R-R/K-X-S*/T*
R-X_2-S*/T*
R-X-S*/T*

B

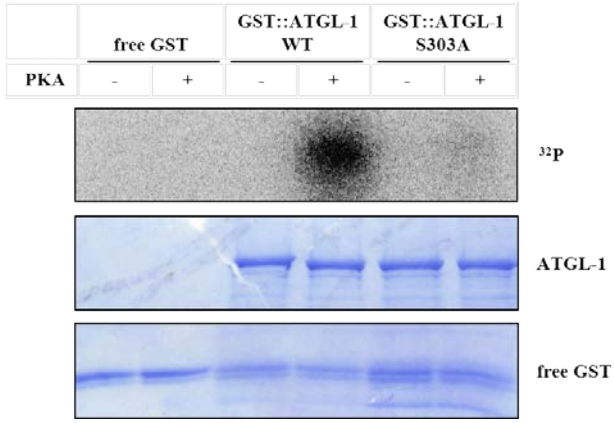

Figure 4. Phosphorylation at serine 303 regulates ATGL-1 protein expression.

HEK 293T cells were maintained in DMEM medium supplemented with 10% FBS. (A) HEK 293T cells were transfected with WT, S303A, or S303D Flag-tagged atgl-1. After incubation for 20 hours, 20 μM forskolin was treated with serum-free DMEM media for 4 hours. Nuclear fractions were analyzed by Western blotting with either FLAG or β-actin antibodies. (B) The relative ATGL-1 protein levels were quantified using the Image J software (NIH) and each protein level was normalized by β-actin.

Figure 4

A

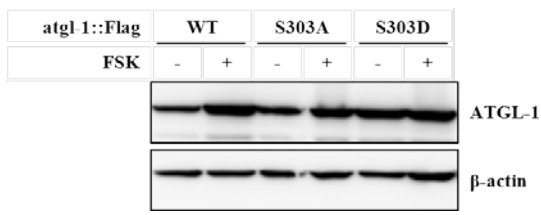
atgl-1::Flag
WT
S303A
S303D
FSK
- + - + - +
ATGL-1
β-actin

B

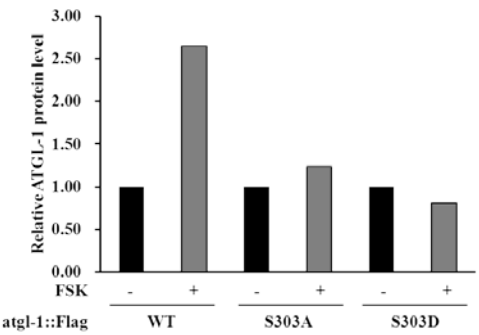
Relative ATGL-1 protein level
3.00
2.50
2.00
1.50
1.00
0.50
0.00
FSK
- + - + - +
atgl-1::Flag
WT
S303A
S303D

mutant (Fig. 2A). On the contrary, both phosphorylation-defective (S303A) and phospho-mimic (S303D) showed only a slight increase upon forskolin treatment (Fig. 4A and B). It appears that the protein level of S303A was not increased because it could not be phosphorylated while that of S303D was not elevated because it was already negatively charged, mimicking the effect of phosphorylation. However, since the protein level of S303A is still slightly increased upon forskolin treatment, it is likely that phosphorylation at serine 303 is not the only mechanism that could regulate ATGL-1 protein level. This unresponsiveness to forskolin of both mutants suggests that phosphorylation at serine 303 by PKA might regulate the level of ATGL-1 protein.

Phosphorylation at serine 303 regulates the level of ATGL-1 protein partially through protein degradation

There are several possible ways to regulate protein level, such as post-transcriptional regulation, translational regulation, post-translational modification (PTM), or protein degradation by proteasome. Among these various regulatory mechanisms, I first focused on the regulation of ATGL-1 protein level by degradation. To investigate the effect of serine 303 phosphorylation on ATGL-1 protein stability, I overexpressed WT and S303A ATGL-1 in HEK 293T cells and simultaneously treated forskolin with or without MG132, a proteasome inhibitor.

Upon forskolin, the protein level of WT ATGL-1 was increased as expected (Fig. 5A and B). When MG132 was treated, the protein level of WT ATGL-1 was also elevated under basal state (no forskolin treated) but did not change in forskolin-stimulated state (Fig. 5A and B). Therefore, it seems that ATGL-1 is being degraded by proteasome in

Figure 5. Phosphorylation at serine 303 regulates the level of ATGL-1 protein partially through protein degradation.

HEK 293T cells were maintained in DMEM medium supplemented with 10% FBS. (A) HEK 293T cells were transfected with WT, S303A, or S303D Flag-tagged atgl-1. After incubation for 20 hours, 20 μM forskolin (FSK) and/or 20 μM MG132 were treated with serum-free DMEM media for 4 hours. Nuclear fractions were subjected to Western blot analysis with either FLAG or β-actin antibodies. (B) The relative ATGL-1 protein levels were quantified using the Image J software (NIH) and each protein level was normalized by β-actin. Values are mean ± S.D. (n=2 for each group). #$p<0.05$, ##$P<0.01$ versus same DNA construct in control state. Student′s t-test.

Figure 5

A

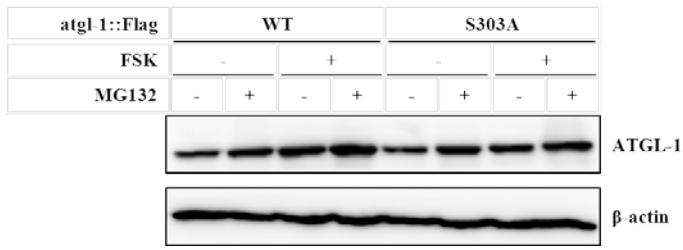
atgl-1::Flag
WT
S303A
FSK
MG132
ATGL-1
β-actin

B

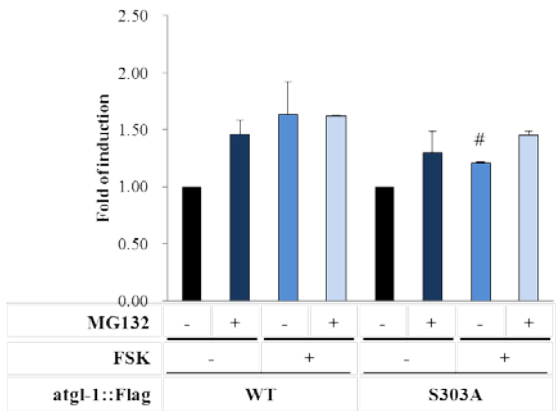
2.50
2.00
1.50
1.00
0.50
0.00
Fold of induction
#
MG132
FSK
atgl-1::Flag
WT
S303A

basal state, but when it gets phosphorylated at serine 303, the phosphorylation somehow stabilizes ATGL-1 and prevents it from degradation by proteasome. In contrast to WT ATGL-1, S303A ATGL-1 protein level was only slightly increased by forskolin (Fig. 5A and B) as previously observed (Fig. 4A and B). In basal state, treatment of MG132 increased the protein level of S303A ATGL-1 to an extent similar to that of WT ATGL-1. This result indicates that in basal state, when ATGL-1 is not phosphorylated by PKA, ATGL-1 protein would be readily degraded by proteasome. However, in forskolin-stimulated condition, S303A ATGL-1 protein level was increased by MG132 treatment, unlike WT ATGL-1 (Fig. 5A and B). Together, these data suggest that phosphorylation at serine 303 could affect ATGL-1 protein by regulating ATGL-1 protein stability and/or its degradation by proteasome.

Phosphorylation at serine 303 regulates ATGL-1 protein expression *in vivo*

To test the effect of phosphorylation on ATGL-1 protein level *in vivo*, I investigated the patterns of WT or S303A ATGL-1::GFP expression upon kin-2 knockdown in *C. elegans*. In order to do this, I generated WT or S303A ATGL-1 transgenic worms by microinjection and fed kin-2 RNAi. The amount of GFP puncta of WT worm was greatly increased upon kin-2 knockdown, as previously observed with VS20 strain (Fig. 6). On the other hand, the amount of GFP puncta of S303A mutant was also enhanced upon kin-2 knockdown, but to a less degree than WT worm (Fig. 6). This result is consistent with *in vitro* data, in which the protein level of S303A ATGL-1 was increased by forskolin treatment but not as much as that of WT ATGL-1 (Fig. 4A and B, 5A and B). These data reveal that phosphorylation at serine 303 of ATGL-1 by PKA

would regulate ATGL-1 protein level in *C. elegans*.

Figure 6. Phosphorylation at serine 303 regulates ATGL-1 protein expression *in vivo*. Transgenic worms overexpressing either GFP-tagged WT or GFP-tagged S303A atgl-1 were grown on L4440 or kin-2 RNAi plates for 2 to 3 days until gravid young adult stage. The GFP fluorescence was visualized using a Zeiss Axio Observer Z1 microscope equipped with Zeiss LSM 700 confocal under EGFP and Nile Red filters. For image analyses, images were captured using Zeiss Zen 2009 software. All images were obtained under identical settings and exposure time. n=5 for each group.

Figure 6

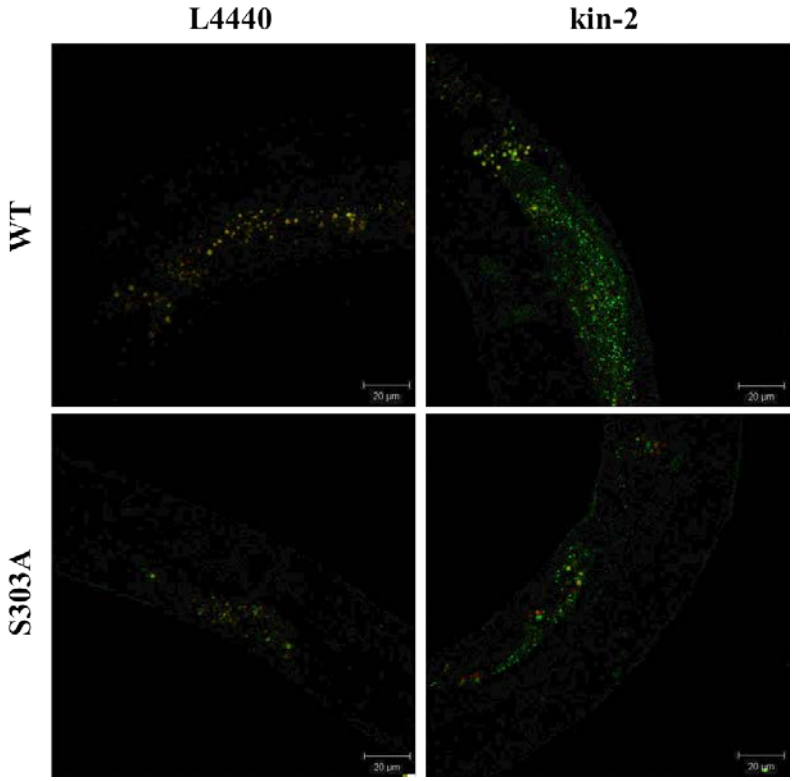

DISCUSSION

In this study, I have investigated the relationship between ATGL-1 and PKA and the effect of phosphorylation by PKA on ATGL-1 protein level in *C. elegans*. Atgl-1 (C05D11.7) and kin-1/2 (ZK909.2 and R07E4.6, respectively) have been previously identified as *C. elegans* homolog of ATGL and PKA, respectively, and they have been implicated in fasting lipolysis without mechanistic understanding. Since the lipolytic machinery of *C. elegans* is distinct from that of mammals, the regulatory mechanism of ATGL and its relationship with PKA may not be the same as mammals. Here, I propose that PKA is an upstream factor of ATGL-1 and directly regulates ATGL-1 protein level by phosphorylation in *C. elegans*.

I observed that PKA acts at upstream level of ATGL-1 and is able to directly regulate it mainly at protein level rather than mRNA level (Fig. 1 and 2). Although these data were obtained using transgenic mutants such as KG532 and VS20, the fact that endogenous atgl-1 mRNA level was not significantly changed during fasting in N2 worms suggests that PKA does not primarily regulate ATGL-1 at mRNA level but at protein level (Fig. 2C).

In vitro kinase assay revealed that PKA primarily phosphorylates ATGL-1 at serine 303. When serine 303 was mutated to alanine, the phosphorylation of ATGL-1 was almost completely disappeared (Fig. 3B). However, it was not completely abrogated for S303A ATGL-1, indicating that phosphorylation at other sites may be further involved for regulatory process (Fig. 3B). For instance, there are other serine residues such as serine 316 that achieved high scores when potential sites were predicted by GPS2.1 (Fig. 3A).

Mammalian ATGL was also shown to be phosphorylated at two sites (serine 404 and serine 428 for humans, serine 406 and serine 430 for mouse) by phospho-protein proteomic mass spectrometry analysis (Bartz *et al*, 2007). Therefore, the phosphorylation status of other predicted sites and their potential effect on ATGL-1 would require further investigation. The phosphorylation of ATGL-1 by PKA was observed only *in vitro*; however, the increase of ATGL-1::GFP in VS20 strain and the relatively less increase in S303A transgenic worm upon kin-2 knockdown suggest that phosphorylation might also occur *in vivo*. Furthermore, although the PKA used in the *in vitro* kinase assay was originated from mammalian gene, *C. elegans* PKA bears approximately 60% sequence homology to mammalian PKA, making it one of the best conserved gene in *C. elegans*, and the functional domains are well conserved. Therefore, it is possible that endogenous ATGL-1 might be also phosphorylated by endogenous PKA in *C. elegans*.

The serine 303 phosphorylation increases ATGL-1 protein level partially by regulating its protein stability. Upon forskolin treatment, the protein level of WT ATGL-1 was increased by approximately 2.7-fold, but that of S303A ATGL-1 was increased by only 1.3-fold (Fig. 4A and B). This was also confirmed *in vivo*; upon kin-2 knockdown, the amount of GFP puncta of ATGL-1 S303A mutant did not increase as much as that of WT ATGL-1 mutant (Fig. 6). Thus, the serine 303 phosphorylation status of ATGL-1 seems to determine the protein level of ATGL-1. Among many possible mechanisms of protein level regulation, I have focused on protein stability and degradation. The protein level of WT ATGL-1 was increased upon forskolin treatment but was not further induced by co-treatment of MG132 (Fig. 5A and B). On the contrary, the protein level of S303A ATGL-1 was further increased by co-treatment of forskolin and MG132 compared to

forskolin-alone treated group (Fig. 5A and B). These data indicate that at basal level ATGL-1 is degraded by proteasome but when serine 303 is phosphorylated, ATGL-1 becomes stable and therefore ATGL-1 protein increases. However, the protein level of S303A ATGL-1 was still slightly increased upon forskolin treatment. Therefore, it is likely that phosphorylation at other sites may further contribute to ATGL-1 protein regulation. Also, S303A protein was only slightly increased by co-treatment of forskolin and MG132 compared to forskolin alone, suggesting that there might be other mechanisms besides proteasome degradation by which serine 303 phosphorylation could regulate ATGL-1 protein level. The exact mechanism of ATGL-1 protein modulation should be further elucidated by examining other aspects such as post-transcriptional regulation and translational regulation. Furthermore, in Figure 5A and B, the fold of increase of WT ATGL-1 by forskolin was not as great as that previously observed in Figure 4A and B. This discrepancy can be due to variations in experimental settings, such as forskolin treatment duration and cell status.

The mechanism of ATGL-1 phosphorylation and protein level regulation proposed in this work is summarized in Figure 7. In basal state, unphosphorylated ATGL-1 is constantly being degraded by proteasome. However, upon fasting, PKA is activated and phosphorylates ATGL-1 at serine 303 and possibly at other sites as well. Serine 303 phosphorylation prevents ATGL-1 protein from being degraded by proteasome, leading to increase in ATGL-1 protein level.

Phosphorylation by PKA may regulate ATGL-1 in other aspects besides protein level. One such aspect would be ATGL-1 binding affinity with LID-1. In mammals, ATGL is well known to bind with CGI-58 (Granneman *et al*, 2007), and our group has

also observed that ATGL-1 binds with LID-1 (unpublished data). In mammals, it is speculated that binding with CGI-58 mediates ATGL activity as the co-localization of ATGL and CGI-58 is increased upon hormonal stimulation (Granneman *et al*, 2007). Thus, phosphorylation by PKA may affect ATGL-1 binding with LID-1 and possibly alter ATGL-1 hydrolase activity. Phosphorylation and the consequent protein level increase may also affect ATGL-1 translocation to LD and TG hydrolase activity. Previously, it has been reported that the degree of ATGL distribution between the cytosol and the LDs does not change upon fasting stimulus (Zimmerman *et al*, 2004; Granneman *et al*, 2007). Similarly, ATGL phosphorylation does not change ATGL localization on LD (Pagnon *et al*, 2012). However, our group has observed that ATGL-1 not only increases in amount but also translocates more to LD upon fasting in VS20 mutant (unpublished data). Thus, it is plausible that ATGL-1 translocation mechanism and physiological relevance would be different between *C. elegans* and mammals as their conserved lipolytic proteins and processes are different. For example, in mammals, phosphorylation of perilipin at serine 517 is essential for ATGL activation (Miyoshi *et al*, 2007). However, *C. elegans* lacks homologs of perilipin or any other PAT domain-containing LD proteins. In this aspect, it appears that phosphorylation and the consequent increase in protein level stimulate more ATGL-1 translocation to LD. If more ATGL-1 is localized on LD, it may lead to higher TG hydrolase activity. Mammalian ATGL phosphorylation alters the TG hydrolase activity despite no change in cellular localization (Pagnon *et al*, 2012). If the effect of phosphorylation on ATGL-1 hydrolase activity can be elucidated, it will confer a physiological meaning to ATGL-1 phosphorylation by PKA in *C. elegans*. Interestingly, it has been reported that serine 303 of ATGL-1 is also phosphorylated by AAK-1, which

leads to reduced lipolysis (Narbonne *et al*, 2008), implying AMPK and PKA might compete for serine 303 phosphorylation to regulate ATGL-1 hydrolase activity and lipolysis upon stimulus.

Collectively, I suggest that in *C. elegans*, PKA phosphorylates ATGL-1 at serine 303 and this phosphorylation regulates ATGL-1 protein level partially by modulating protein stability. This is the first report of *C. elegans* ATGL-1 phosphorylation by PKA and also the first report of protein level regulation of ATGL/ATGL-1 by PKA phosphorylation. Interestingly, it has been previously reported that CaSR (calcium-sensing receptor) downregulates PKA activity and also reduces ATGL protein amount in human fibroblast (He *et al*, 2011). Thus, it hints that ATGL protein level regulation by PKA phosphorylation reported here might be a mechanism evolutionarily conserved from *C. elegans* to mammal. ATGL is a key enzyme for lipolysis and therefore the results of this study would help advancing our understanding of how lipolysis is regulated and how it has evolved.

Figure 7. PKA phosphorylates and regulates ATGL-1 protein level.

A working model of regulation of ATGL-1 by PKA phosphorylation. In basal state, unphosphorylated ATGL-1 is constantly being degraded by proteasome. Upon fasting, PKA is activated and phosphorylates ATGL-1 at serine 303 and possibly at other sites as well. Serine 303 phosphorylation prevents ATGL-1 protein from being degraded by proteasome, leading to increase in ATGL-1 protein level. PKA phosphorylation may also affect ATGL-1 binding with LID-1 and ATGL-1 translocation to lipid droplets.

Figure 7

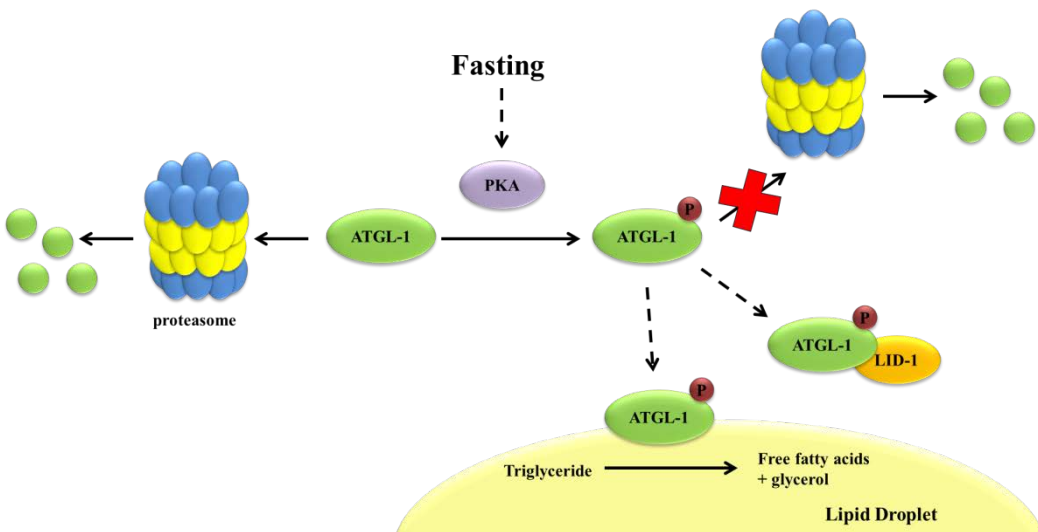
Fasting
PKA
ATGL-1
ATGL-1
P
proteasome
ATGL-1
P
LID-1
ATGL-1
P
Triglyceride
Free fatty acids
+ glycerol
Lipid Droplet

REFERENCES

Bartz, R., Zehmer, J.K., Zhu, M., Chen, Y., Serrero, G., Zhao, Y., Liu, P. (2007) Dynamic activity of lipid droplets: protein phosphorylation and GTP-mediated protein translocation. J. Proteome. Res. 6, 3256–3265.

Brasaemle,D.L.,Dolios, G., Shapiro, L., Wang, R. (2004) Proteomic analysis of proteins associated with lipid droplets of basal and lipolytically stimulated 3T3-L1 adipocytes. J. Biol. Chem. 279, 46835–46842.

Fain, J.N., Saperstein, R. (1970) The involvement of RNA synthesis and cyclic AMP in the activation of fat cell lipolysis by growth hormone and glucocorticoids. Horm. Metab. Res. 2 (Suppl 2), 20-27.

Fischer, J., Lefevre, C., Morava, E., Mussini, J.M., Laforet, P., Negre-Salvayre, A., Lathrop, M., Salvayre, R. (2007) The gene encoding adipose triglyceride lipase (PNPLA2) is mutated in neutral lipid storage disease with myopathy. Nat. Genet. 39, 28–30.

Fredrikson, G., Stralfors, P., Nilsson, N.O., Belfrage, P. (1981) Hormone-sensitive lipase of rat adipose tissue. Purification and some properties. J. Biol. Chem. 256, 6311-6320.

Fujimoto, Y., Itabe, H., Kinoshita, T., Homma, K.J., Onoduka, J., Mori, M., Yamaguchi,

S., Makita, M., Higashi, Y., Yamashita, A. (2007) Involvement of ACSL in local synthesis of neutral lipids in cytoplasmic lipid droplets in human hepatocyte HuH7. J. Lipid Res. 48, 1280-1292.

Granneman, J.G., Moore, H.P., Granneman, R.L., Greenberg, A.S., Obin, M.S., Zhu, Z. (2007) Analysis of lipolytic protein trafficking and interactions in adipocytes. J. Biol. Chem. 282, 43615-43619.

Haemmerle, G., Zimmermann, R., Hayn, M.,Theussl, C.,Waeg, G., Wagner, E., Sattler, W.,Magin, T.M., Wagner, E. F.,Zechner, R. (2002) Hormone-sensitive lipase deficiency in mice causes diglyceride accumulation in adipose tissue, muscle, and testis. J. Biol. Chem. 277, 4806–4815.

Haemmerle, G., Lass, A., Zimmermann, R., Gorkiewicz, G., Meyer, C., Rozman, J., Heldmaier, G., Maier, R., Theussl, C., Eder, S., Kratky, D., Wagner, E.F., Klingenspor, M., Hoefler, G., Zechner, R. (2006) Defective lipolysis and altered energy metabolism in mice lacking adipose triglyceride lipase. Science 312, 734–737.

He, Y., Zhang, H., Teng, J., Huang, L., Li, Y.,Sun, C. (2011) Involvement of calcium-sensing receptor in inhibition of lipolysis through intracellular cAMP and calcium pathways in human adipocytes. Biochem Biophys Res Commun. 404, 393-399.

Heckemeyer, C.M., Barker, J., Duckworth, W.C., Solomon, S.S. (1983) Studies of the

biological effect and degradation of glucagon in the rat perifused isolated adipose cell. Endocrinology 113, 270-276.

Hirsch, A. H., Rosen, O. M. (1984)Lipolytic stimulation modulates the subcellular distribution of hormone-sensitive lipase in 3T3-L1 cells. J. Lipid Res. 25, 665–677.

Jenkins, C. M.,Mancuso, D. J., Yan, W., Sims, H. F., Gibson, B., Gross, R. W. (2004) Identification, cloning, expression, and purification of three novel human calcium-independent phospholipase A2 family members possessing triacylglycerol lipase and acylglyceroltransacylase activities. J. Biol. Chem. 279, 48968–48975.

Kennelly, P.J., Krebs, E.G. (1991) Consensus Sequences as Substrate Specificity Determinants for Protein Kinases and Protein Phosphatases. J Biol. Chem. 266, 15555-15558.

Lass,A., Zimmermann, R., Haemmerle, G., Riederer, M., Schoiswohl, G., Schweiger, M., Kienesberger, P., Strauss, J.G., Gorkiewicz, G., Zechner, R. (2006) Adipose triglyceride lipase mediated lipolysis of cellular fat stores is activated by CGI-58 and defective in Chanarin–Dorfman Syndrome. Cell. Metab.3, 309–319.

Lefevre, C., Jobard, F., Caux, F., Bouadjar, B., Karaduman, A., Heilig, R., Lakhdar, H., Wollenberg, A., Verret, J.L., Weissenbach, J., Ozguc, M., Lathrop, M., Prud, J.F., Fischer, J. (2001) Mutations in CGI-58, the gene encoding a new protein of the

esterase/lipase/thioesterase subfamily, in Chanarin–Dorfman Syndrome. Am. J. Hum. Genet. 69, 1002–1012.

Liu, P., Ying, Y., Zhao, Y., Mundy, D. I., Zhu, M., Anderson, R. G. (2004) Chinese hamster ovaryK2 cell lipid droplets appear to be metabolic organelles involved in membrane traffic. J. Biol. Chem. 279, 3787–3792.

Miyoshi, H., Perfield 2nd, J.W., Souza, S.C., Shen, W.J., Zhang, H.H., Stancheva, Z.S., Kraemer, F.B., Obin, M.S., Greenberg, A.S. (2007) Control of adipose triglyceride lipase action by serine 517 of perilipin A globally regulates protein kinase A-stimulated lipolysis in adipocytes.J. Biol. Chem. 282, 996-1002.

Mullaney, B.C., Ashrafi, K. (2009) C. elegans fat storage and metabolic regulation. Biochimica Biophysica Acta. 1791, 474-478.

Murphy, D.J., Vance J. (1999) Mechanisms of lipid-body formation. Trends Biochem. Sci. 24, 109-115.

Narbonne, P., Roy, R. (2008) *Caenorhabditis elegans* dauers need LKB1/AMPK to ration lipid reserves and ensure long-term survival. Nature 457, 210-214.

O'Rourke, E.J., Soukas, A.A., Carr, C.E., Ruvkun, G. (2009) *C. elegans* Major Fats are stored in vesicles distinct from Lysosome-Related Organelles. Cell Metab. 10, 430-435.

Ohsaki, Y., Cheng, J., Suzuki, M., Shinohara, Y., Fujita, A., Fujimoto, T. (2009) Biogenesis of cytoplasmic lipid droplets: From the lipid ester globule in the membrane to the visible structure. Biochim. Biophys. Acta 1791, 399-407.

Pagnon, J., Matzaris, M., Stark, R.,Meex, R.C.R., Macaulay, S. L., Brown, W., O'Brien, P.E.,Tiganis, T., Watt, M.J. (2012) Identification and Functional Characterization of Protein Kinase A Phosphorylation Sites in the Major Lipolytic Protein, Adipose Triglyceride Lipase. Endocrinology 153, 4278-4289.

Perea, A., Clemente, F., Martinell, J., Villanueva-Penacarrillo, M.L. Valverde, I. (1995) Physiological effect of glucagon in human isolated adipocytes. Horm. Metab. Res. 27, 372-375.

Robenek, H., Hofnagel, O., Buers, I., Robenek, M.J., Troyer, D., Severs, N.J. (2006) Adipophilin-enriched domains in the ER membrane are sites of lipid droplet biogenesis. J. Cell Sci. 119, 4215-4224.

Schroeder, L.K., Kremer, S., Kramer, M.J., Currie, E., Kwan, E., Watts, J.L., Lawrenson, A.L., Hermann, G.J. (2007) Function of the Caenorhabditis elegans ABC transporter PGP-2 in the biogenesis of a lysosome-related fat storage organelle. Mol. Biol. Cell 18, 995-1008.

Slavin, B.G., Ong, J.M., Kern, P.A. (1994) Hormonal regulation of hormone-sensitive lipase activity and mRNA levels in isolated rat adipocytes. J. Lipid Res. 35, 1535-1541.

Sourkas, A.A., Kane, E.A., Carr, C.E. (2009) Rictor/TORC2 regulates fat metabolism, feeding, growth, and lifespan in *Caenorhabditis elegans*. Genes Dev. 23, 496-511.

Steinberg, D., Huttunen, J. K. (1972) The role of cyclic AMP in activation of hormone sensitive lipase of adipose tissue. Adv. Cyclic Nucleotide Res. 1, 47–62.

Steinberg, G.R., Kemp, B.E., Watt, M.J. (2007) Adipocyte triglyceride lipase expression in human obesity. Am. J. Physiol. Endocrinol. Metab. 293, E958-E964.

Subramanian, V., Rothenberg, A., Gomez, C., Cohen, A.W., Garcia, A., Bhattacharyya, S., Shapiro, L., Dolios, G., Wang, R., Lisanti, M.P., Brasaemle, D.L. (2004) Perilipin A mediates the reversible binding of CGI-58 to lipid droplets in 3T3-L1 adipocytes. J. Biol. Chem. 279, 42062-42071.

Timmons, L., Fire, A. (1998) Specific interference by ingested dsRNA. Nature 395, 854.

Villena, J.A., Roy, S., Sarkadi-Nagy, E., Kim, K.H., Sul, H. S. (2004) Desnutrin, an adipocyte gene encoding a novel patatin domain-containing protein, is induced by fasting and glucocorticoids: ectopic expression of desnutrin increases triglyceride hydrolysis. J. Biol. Chem. 279, 47066–47075.

Xu, C., He, J., Jiang, H., Zu, L., Zhai, W., Pu, S. (2009) Direct effect of glucocorticoids on lipolysis in adipocytes. Mol Endocrinol 23, 1161-1170.

Xue Y., Ren J., Gao X., Jin C., Wen L., Yao X. (2008) GPS 2.0, a Tool to Predict Kinase-specific Phosphorylation Sites in Hierarchy. Mol Cell Proteomics 7, 1598-1608.

Yamaguchi, T., Omatsu, N., Matsushita, S., Osumi, T. (2004) CGI-58 interacts with perilipin and is localized to lipid droplets. Possible involvement of CGI-58 mislocalization in Chanarin-Dorfman Symdrome. J. Biol. Chem. 279, 30490-30497.

Yeaman, S.J., Smith, G.M., Jepson, C.A., Wood, S.L., Emmison, N. (1994) Themultifunctional role of hormone-sensitive lipase in lipid metabolism. Adv. Enzyme Regul. 34, 355-370.

Zimmermann, R., Strauss, J. G., Haemmerle, G., Schoiswohl, G., Birner-Gruenberger, R., Riederer, M., Lass, A., Neuberger, G., Eisenhaber, F., Hermetter, A., Zechner, R. (2004) Fat mobilization in adipose tissue is promoted by adipose triglyceride lipase. Science 306, 1383–1386.

Zimmermann, R., Lass, A., Haemmerle, G., Zechner, R. (2009) Fate of fat: The role of adipose triglyceride lipase in lipolysis. Biochimica Biophysica Acta 1791, 494-500.

국문 초록

PKA에 의한 예쁜꼬마선충 ATGL-1 단백질 양적 조절

장 주 연

생명과학부

서울대학교

절식으로 인한 지방분해는 저장된 지방 대사물을 가수분해하여 에너지원을 제공하는 과정에서 중요한 역할을 한다. 예쁜꼬마선충에도 Adipose Triglyceride Lipase-1 (ATGL-1)과 Protein Kinase A (PKA)는 잘 보존되어 있으며 지방분해에 관여한다고 알려져 있다. 하지만 예쁜꼬마선충에서 ATGL-1 의 조절 기전과 PKA 와의 상호기능적 연관성에 대하여 알려진 바가 거의 없다. 본 연구에서는 ATGL-1 이 PKA 에 의한 지방분해에 필요하며 PKA 가 ATGL-1 의 세린 303 번 기 (serine 303)를 인산화시킨다는 것을 규명하였다. 또한, ATGL-1 의 인산화가 ATGL-1 단백질의 양적 조절에 연관되어 있음을 밝혔다. 이러한 인산화에 의한 ATGL-1 의 양적 조절은 단백질 안정성을 조절함으로써 이루어졌지만, 다른 기전이 관여할 가능성도 배제할 수 없다.

결론적으로, 본 연구 결과는 PKA 인산화에 의한 ATGL-1 단백질의 양적 조절 기전에 대한 새로운 모델을 제시하고 있으며, 이러한 기전은 절식 과정에서 ATGL-1 에 의한 지방분해 과정에 중요하게 작용할 것으로 예상된다.

주요어: ATGL-1, PKA, 인산화, 단백질 양적 조절

학번: 2011-23260

감사의 글

짧다면 짧고 길다면 긴 2년, 아니 인턴 기간까지 포함해서 2년 반 정도의 시간이 벌써 끝이 났습니다. 처음 들어올 때는 멀게만 느껴지던 졸업이었는데 벌써 끝이라니 실감이 나지 않지만 한편으론 감회가 새롭습니다. 지난 2년 반 동안 실험실에서의 생활은 여러모로 저에게 소중한 경험이었습니다. 지금의 저를 있게 해준 모든 분들께 감사의 인사를 드리고 싶습니다.

우선 저를 지난 2년 반 동안 격려해주시고 이끌어주신 김재범 교수님께 가장 먼저, 가장 큰 인사를 올려야 할 것 같습니다. 저를 믿어주시고 늘 격려와 충고 아끼지 않아주신 점 늘 감사하게 생각하고 있습니다. 교수님이 물심양면으로 도와주신 것 절대 잊지 않고 사회에 나가서도 선생님과 실험실 이름을 빛낼 수 있는 사람이 되도록 노력하겠습니다.

또한 예쁜꼬마선충 연구를 하는데 있어 필요한 재료와 장비를 제공해주신 이준호 교수님 감사드립니다. 더불어 잘 모르는 석사과정생의 논문 심사를 흔쾌히 허락해주신 정종경 교수님께도 감사드립니다.

그리고 LAMR 식구들에게도 감사인사 드립니다. 제일 먼저 저를 2년 반 동안 맡아 수고 많으셨던 이정현 오빠에게 감사하다고 말하고 싶습니다. 다른

사람들이 말한 것처럼 많은 배려 해주신 좋은 사수 만나 실험도 잘 배우고 연구실 생활 즐겁게 하다 갈 수 있었습니다. 그리고 정현 오빠와 함께 저에게 실험도 가르쳐주고 넉살이 좋아 마음 편하게 대해준 공진욱에게도 고맙다고 말하고 싶습니다. 또한 저에게 먼저 다가와주고 편히 대해준 장하군 오빠와 졸업 준비 하는데 여러모로 도움과 조언 주고 마지막 실험도 자기 일처럼 도와준 이재호 오빠께도 감사 드립니다. 그 외에도 항상 밝고 부드러우신 성격으로 배울 점이 많았던 가소정 박사님, 미팅 때 좋은 코멘트 많이 해주신 최성식 오빠, 저와 함께 안에서 밥 먹으며 얘기 나눈 이가영 박사님, 허진영 언니, 함미라 언니, 항상 실험 열심히 하시는 김아영 언니, 실험실의 엔도르핀이 되시는 황인재 오빠와 박윤정 언니, 항상 친절하게 대해주시고 특히 한라산에서 저를 도와주신 김종인 오빠, 실험실에서나 MT 가서나 항상 솔선수범하셔서 귀감이 되신 신경철 오빠, 실험실의 궂은 일 도맡아 해준 이궁 오빠, 최원근, 손지형, 그리고 저희가 편히 실험할 수 있도록 항상 많이 도와주시는 송민선 언니에게도 감사 인사 전합니다.

함께 서울 올라와 자주는 못 만나도 만날 때마다 내게 힘이 되어준 권은지, 김도연, 박주연, 한상인, 황진영도 모두 고맙다. 내가 제일 먼저 떠나지만, 어디에 있든 항상 지금처럼 서로 생각해주고 격려하면서 살아가자. 그리고 항상 연락해야지 하면서 못했었는데 먼저 잊지 않고 연락해준 다른 학부 시절 친구들도 모두 고마워.

마지막으로 항상 저를 뒷바라지해주고 응원해준 저희 가족에게 감사드립니다. 제 불평불만 들어주고 반찬 만들어주느라 고생하신 엄마, 사회생활 조언해주시는 아빠, 그리고 저를 챙겨주고 도와주는 언니에게 모두 감사드립니다.

이 모든 분들이 있었기에 훗날 뒤돌아봤을 때 제 대학원 시절이 좋은 추억으로 남을 것 같습니다. 모두 다시 한 번 감사드리고, 서로 다른 길을 가더라도 각자의 자리에서 멋진 삶 만들어나가길 기원합니다.

장 주 연